Improved doxorubicin encapsulation and pharmacokinetics of ferritin-fusion protein nanocarriers bearing PAS elements

Journal:	*Biomacromolecules*
Manuscript ID	Draft
Manuscript Type:	Article
Date Submitted by the Author:	n/a
Complete List of Authors:	Falvo, Elisabetta; CNR – National Research Council of Italy, Institute of Molecular Biology and Pathology; University "La Sapienza" Rome, Dept. Biochemical Sciences Tremante, Elisa; Regina Elena National Cancer Institute, Immunology Arcovito, Alessandro; Università Cattolica del Sacro Cuore, Istituto di Biochimica e Biochimica Clinica Papi, Massimiliano; Università Cattolica del SC, Physics Elad, Nadav; Department of Chemical Research Support, Weizmann Institute of Science, Rehovot, Israel Boffi, Alberto; University "La Sapienza" Rome, Dept. Biochemical Sciences Morea, Veronica; Consiglio Nazionale delle Ricerche, Istituto di Biologia e Patologia Molecolari Conti, Giamaica; University of Verona, Toffoli, Giuseppe; Centro di Riferiemento Oncologico, IRCCS, National Cancer Institute, Experimental and Clinical Pharmacology Fracasso, Giulio; University of Verona, Giacomini, Patrizio; Regina Elena National Cancer Institute, Immunology Ceci, Pierpaolo; CNR – National Research Council of Italy, Institute of Molecular Biology and Pathology,

Improved doxorubicin encapsulation and pharmacokinetics of ferritin-fusion protein nanocarriers bearing PAS elements

Elisabetta Falvo[1,2,], Elisa Tremante[3], Alessandro Arcovito[4], Massimiliano Papi[5], Nadav Elad[6], Alberto Boffi[1,2,7], Veronica Morea[1], Giamaica Conti[8], Giuseppe Toffoli[9], Giulio Fracasso[10], Patrizio Giacomini[3], Pierpaolo Ceci[1,*]*

[1] CNR – National Research Council of Italy, Institute of Molecular Biology and Pathology, Rome (Italy)

[2] Department of Biochemical Sciences "A. Rossi Fanelli", University "Sapienza", Rome, Italy

[3] Immunology Laboratory, National Cancer Institute Regina Elena, Rome, Italy

[4] Istituto di Biochimica e Biochimica Clinica, Università Cattolica del Sacro Cuore, Largo F. Vito 1, 00168, Rome, Italy

[5] Istituto di Fisica, Università Cattolica del Sacro Cuore, Largo F. Vito 1, 00168, Rome, Italy

[6] Department of Chemical Research Support, Weizmann Institute of Science, Rehovot, Israel

[7] Center for Life Nano Science at Sapienza, Istituto Italiano di Tecnologia (IIT), Rome, Italy

[8] Department of Neurological and Movement Sciences, University of Verona, Verona, Italy

[9] Experimental and Clinical Pharmacology Unit, CRO-National Cancer Institute, AVIANO - PN - Italy

[10] Department of Medicine, University of Verona, Italy

Corresponding Authors

* pierpaolo.ceci@cnr.it; elisabetta.falvo@uniroma1.it

Keywords: protein-based nanocarrier; ferritin; PASylation; doxorubicin encapsulation; pharmacokinetics; drug-delivery

ABSTRACT. A novel human ferritin-based nanocarrier, composed of 24 modified monomers able to auto-assemble into a modified protein cage, was produced and used as selective carrier of anti-tumor payloads. Each modified monomer derives from the genetic fusion of two distinct modules, namely the heavy chain of human ferritin (HFt) and a stabilizing/protective PAS polypeptide sequence rich in proline (P), serine (S) and alanine (A) residues. Two genetically fused protein constructs containing PAS polymers with 40 and 75 residue length were compared. They were produced and purified as recombinant proteins in *Escherichia coli* at high yields. Both preparations were highly soluble and stable *in vitro* as well as in mouse plasma. Size-exclusion chromatography, dynamic light scattering and transmission electron microscopy results indicated that PASylated ferritins are fully assembled and highly monodispersed. In addition, yields and stability of encapsulated Doxorubicin were significantly better for both HFt-PAS proteins than

wild-type HFt. Importantly, PAS sequences considerably prolonged the half-life of HFt in the mouse bloodstream. Finally, our doxorubicin-loaded nanocages preserved the pharmacological activity of the drug. Taken together, these results indicate that both the developed HFt-PAS fusion proteins are promising nanocarriers for future applications in cancer therapy.

INTRODUCTION

Protein-cage molecules based on ferritins (Fts) are attracting growing interest in the field of drug-delivery, due to their exceptional characteristics, namely biodegradability, solubility, functionalization versatility and remarkable capacity to bind different types of drugs.[1-11] Ferritin is a highly symmetrical multimeric protein consisting of 24 subunits that self-assemble into a shell-like sphere, with external and internal diameters of 12 and 8 nm, respectively, enclosing a hollow cavity used for iron storing.

Nanoparticles (NPs) based on the heavy chain of the human protein ferritin (HFt) compare favourably with other systems, particularly for human applications *in vivo*. Indeed, Fts are present, under physiological conditions, both inside cells and, although at low levels (about 20 μg/L), in the bloodstream, where they are stable and soluble. Additionally, Fts are able to pass body barriers and, being natural self constituents, they are likely not to elicit strong non-self antibody and/or T cell immune responses.[12] Several groups, included ourselves, have reported that Fts are effective templates for loading, in their internal cavity, imaging agents for magnetic resonance imaging (MRI), positron emission tomography (PET), organic molecules and drugs.[1-3, 13-18] Further, Fts can be easily functionalized by genetic engineering and/or chemical conjugation involving one of the many chemical groups present on the protein external surface and exposed to solvent (i.e., primary amines, carboxylates, thiols). Of particular relevance, especially in view of potential applications

in cancer therapy, is the ability of HFt to be easily internalized by many types of protein- and "iron-hungry" cancer cells.[19]

In spite of its many advantageous features, two main HFt weaknesses should be tackled to harness its full potential as drug-delivery system.[6] First, HFt plasma half-life after systemic injection (i.e., about 2 hours) may be too short to attain sufficient accumulation at the tumor level, a problem shared by most other first-generation protein therapeutics. Second, although HFt was reported to bind and encapsulate some types of drugs, both the yields and stability of the resulting HFt-drug complexes were not satisfactory. As an example, during the last three years ferritin-doxorubicin complexes have been obtained by several groups, mostly by performing reversible, pH-dependent HFt dissociation (pH 2.0) and reassociation (pH 7.5) in the presence of the drug.[2, 6-7, 20-22] Typically, this process resulted in the loss of more than 50% of the starting protein material and an average of 25-30 doxorubicin molecules encapsulated within each protein cavity. Moreover, more than 30% of the drug leaked by the first week of storage, indicating that the stability of the ferritin-doxorubicin complexes is quite far away from the requirements of the pharmaceutical industry. Therefore, both these issues may hamper the development of HFt-drugs complexes for clinical applications.

To overcome these problems, we have developed a novel HFt-based genetic construct obtained by fusing HFt to a PAS polypeptide sequence, i.e., a sequence rich in proline (P), alanine (A) and serine (S) residues (Scheme 1). In fact, the use of natively disordered PAS polypeptides had been reported to eliminate the disadvantages associated with protein-PEGylation for the development and production of a number of biopharmaceuticals.[23-24] As an example, after synthetic conjugation of PEG molecules with recombinant proteins additional *in vitro* processing and purification steps have to be performed to obtain PEG derivatives with suitably high purity (GMP-grade), and this lowers the yields and raises the manufacturing costs. Conversely, genetic constructs containing

PAS polypeptides are uniquely homogeneous, stable in blood plasma and degradable by kidney enzymes, thus evading organ accumulation, while lacking toxicity or immunogenicity in animal.[23] In this work we investigated two HFt-PAS constructs, whose PAS polymers comprise 40 (HFt-PAS40) and 75 (HFt-PAS75) residues, respectively. In both types of constructs, 24 PAS sequences are exposed on the external surface of the HFt cage, since they are fused to solvent-accessible N-terminal region of HFt. The HFt-PAS constructs were obtained and purified as recombinant proteins in *Escherichia coli* at high yields (100 mg per *E. coli* liter). They resulted to be highly soluble and stable in both buffer and plasma. Size-exclusion chromatography, dynamic light scattering and transmission electron microscopy experiments indicated that HFt-PAS40 and HFt-PAS75 are fully assembled and highly monodispersed with an average diameter of 17 and 20 nm, respectively. Both HFt-PAS proteins resulted to be endowed with higher stability than HFt during the pH jump (2.0-7.5) step performed to encapsulate doxorubicin; moreover they showed a significant increment in drug loading and as well as stability with respect to wild-type HFt. Finally, it is noteworthy that PAS-containing constructs showed considerably longer *in vivo* circulation than HFt in healthy mice. Take together these results indicate that HFt-PAS constructs are more suitable nanocarriers for potential *in vivo* applications than wild-type HFt or PEGylated HFt-derivatives.

EXPERIMENTAL SECTION

Protein structure analysis and modelling. The three-dimensional (3D) structure of HFt, determined by X-ray crystallography, was downloaded from the Protein Data Bank (PDB; www.pdb.org; PDB ID: 3AJO). Protein structure visualization and modelling of PAS chains and glycine-rich linkers were performed using the software InsightII (Accelrys Inc).

Cloning, overexpression and purification of HFt-PAS constructs. The *HFt-PAS40* and *HFt-PAS75* genes were obtained by genetically linking 40- and 75-residues long PAS polypeptides, respectively, with the HFt sequence. PAS and HFt sequences were separated by a linker made of three glycine residues. The expression vectors pET-11a containing the *HFt-PAS40* and *HFt-PAS75* genes were assembled by GENEART AG (Germany). Gene synthesis was performed taking into consideration the codon-optimization for high level expression in *Escherichia coli*. PAS sequences used in this study were the following: ASPAAPAPASPAAPAPSAPAASPAAPAPASPAAPAPSAPAASPAAPAPASPAAPAPSAPAAS PAAPAPASPAAPA (the first 40 residues, underlined, were used for Hft-PAS40). Recombinant HFt and HFt-PAS constructs were expressed and purified from *E. coli*, as previously described for HFt, with the addition of ion exchange chromatography run and one ultracentrifugation step.[1] Samples dialyzed overnight against phosphate buffered saline (PBS) pH 7.5 were loaded on a strong anion exchange column HiTrap Q HP (Q Sepharose High Performance GE Healthcare, Boston, USA) previously equilibrated with the same buffer. In these conditions, HFt samples eluted from the column whereas other *E. coli* proteins and DNA contaminants did not. The recovered HFt samples were ultracentrifugated at 35000 rpm for 55 min at 6 °C using a Beckman L8-70M ultracentrifuge (Beckman Coultier). The recovered supernatant was then precipitated using ammonium sulphate at 65% saturation (w/v). The pellet was resuspended and dialyzed overnight against PBS pH 7.5, pooled and concentrated, by means of 30 KDa Amicon Ultra-15 centrifugal filter devices (Millipore, Billerica, MA, USA). Finally the nanocages were sterile filtered and stored at 4 °C. Typical yields were 100 mg of pure proteins per 1 L of bacteria culture. The purity of all the preparations was assessed by SDS-PAGE running the nanocages on 15% gels and staining the protein with Coomassie brilliant blue. Protein concentrations were determined

spectrophotometrically at 280 nm, using a molar extinction coefficient (on a 24-mer basis) of $4.56x10^5$ M^{-1} cm^{-1} (ProtParam sofware, http//www.expasy.org).

Preparation of PEGylated HFt. HFt solution (2 mg/mL) was incubated with 1.0 mM of 5 KDa methoxypolyethylene glycol maleimide (Sigma-Aldrich) in PBS pH 7.2, at room temperature, for about 1 hour under stirring. Subsequently, sample was filtered and exchanged 5 times with H_2O_{dd} by using 30 kDa Amicon Ultra-15 centrifugal filter devices to remove excess reagents. The PEGylated sample was sterile filtered and stored at 4 °C.

Size exclusion chromatography (SEC) and dynamic light scattering (DLS) analyses. SEC experiments were performed using a Superose 6 gel-filtration column equilibrated with phosphate buffered saline (PBS) at pH 7.4.

DLS experiments were carried out with a Zetasizer Nano S (Malvern Instruments, Malvern, U.K.) equipped with a 4 mW He–Ne laser (633 nm). Measurements were performed at 25 °C, at an angle of 173° with respect to the incident beam. Peak intensity analyses were used to determine the average hydrodynamic diameters (*Z*-average diameter) of the scattering particles. Results are the average of at least five measurements. All samples were prepared at 1 mg/mL in filtered H_2O_{dd}.

All the traces for both SEC and DLS experiments were analysed with Origin 8.0 (Originlab Corporation, Northampton, MA).

Transmission Electron Microscopy (TEM) analysis. 3.5 µl of HFt-nanocarriers samples (0.1 mg/mL) were applied to carbon coated, glow discharged, EM grids and negatively stained with 2% uranyl acetate. Micrographs were recorded on a TVIPS F224HD 2k x 2k CCD camera (Gauting, Germany) using a Tecnai T12 (FEI, Eindhoven), operating at 120 kV.

Circular Dicroism (CD) spectroscopy. CD measurements were carried out using Jasco J-715 CD apparatus. The far-UV CD spectra were recorded at 25°C in a 0.1 cm quartz cuvette on 1 mg/mL protein concentration in 15 mM phosphate buffer.

Doxorubicin encapsulation in the HFt-based nanocarriers. The chemotherapeutic agent doxorubicin (DOXO) was encapsulated using the previously reported HFt disassembly/reassembly method with minor modifications.[7] Briefly, solutions of HFt, HFt-PAS40 or HFt-PAS75 in 0.1 M NaCl, were incubated at pH 2.0 by adding HCl for 10 minutes. Then, doxorubicin hydrochloride was added to the solution at 300:1 molar ratio and the pH was maintained at a value of 2.5 for further 5 min. The pH was then increased up to a value of 8.0 using NaOH. The resulting solution was stirred at room temperature for 30 min and dialyzed o.n. *vs* PBS at pH 7.4 to remove unbound DOXO. After dialysis, solutions were centrifuged at 15.000 rpm for 30 min at 4°C. Supernatant was collected, concentrated through 30 kDa Amicon Ultra-15 centrifugal devices, sterile filtered and stored at 4°C in the dark. The HFt and DOXO content of the samples were then determined using the Lowry method and UV-vis spectroscopy after performing a DOXO extraction step in acidified (0.75 M HCl) isopropanol. A calculated DOXO molar extinction coefficient ε = 12250 $M^{-1}cm^{-1}$ at 485 nm was used.

Stability of the Doxorubicin-bearing HFt-based nanocarriers (HFt-DOXO). The release of DOXO by HFt-based nanocarriers was evaluated every 7 days for 3 months, in different conditions such as PBS pH 7.4 at 4°C and 37 °C. The amount (%) of drug released was evaluated by SEC experiments at two different wavelengths, i.e., 280 nm and 485 nm, simultaneously.

ntiproliferative effects of the HFt-DOXO constructs *in vitro.* PaCa44 human pancreatic tumor cells were kindly provided by prof. A. Scarpa, Department of Diagnostics and Public Health University of Verona, Italy; cells were grown in RPMI 1640 medium added with 2 mM glutamine, 10% of FBS and antibiotics.

PaCa44 cells ($5*10^3$) were seeded, one day before the assay, in 90 µL of complete medium in 96 well culture microplates. The day after, the cells were incubated in triplicate with 10 µL of serial

dilution of the free drug (i.e. DOXO) or the nanosystems under investigation. After 24 hours the supernatant was removed, the cells were washed and finally resuspended in complete RPMI medium. 93 hours after the start of the cell incubation with our formulations the medium was replaced with a new medium supplemented with XTT reagent (Sigma-Aldrich, St Louis, MO, USA), according to the supplier instructions. Finally, after 3 hours of incubation at 37°C cell viability was measured at 450 nm by a microplate reader (VERSAmax, Molecular Devices, Sunnyvale, CA, USA). The percent of cell viability was estimated analyzing the values obtained from treated cells with respect to mock treated cells. To compare the toxicity of the different nanoformulations we evaluated the IC50, the concentration of drug needed to decrease the cell viability by 50%.

Plasma pharmacokinetics (PK) of the HFt-DOXO constructs *in vivo.* HFt-DOXO, HFt-PAS40-DOXO and HFt-PAS75-DOXO) were i.v., injected into BALB/c healthy mice (n = 3 for each group). In parallel, the naked drugs DOXO and INNO-206 were subjected to the same analysis. INNO-206 (aldoxorubicin (6-maleimidocaproyl)hydrazone) is a novel, albumin-binding formulation of DOXO, which was reported to determine significantly reduced adverse events and increased efficacy with respect to DOXO, as well as having better PK properties due to albumin binding.[25]

DOXO doses of 5 mg/Kg were used for all the samples. At various times after injection blood was collected from the tail vein and the plasma was separated and analyzed for DOXO concentration by a previously reported procedure.[6] Briefly, plasma samples (20 μL) were incubated with 200 μL of acidified (0.75 M HCl) isopropanol overnight at −20 °C in the dark to extract DOXO. The mixture was then centrifuged at 13,000 × g for 20 min and the supernatant was loaded onto a 96-well plate (Corning). DOXO concentration was determined by measuring the fluorescence at 485 nm excitation and 590 nm emission, using a multilabel counter model 1420 VICTOR^{3}™

(PerkinElmer, USA). To correct for non specific background, the fluorescence of blood samples from untreated mice was determined. Standard DOXO concentration from 1 to 4,000 nM was used as linear standard curve.

Animal studies were performed according to a protocol approved by the Institutional Animal Care and Use Committee of the Regina Elena Cancer Institute (Italy).

SCHEME 1. Summary of the structure and the synthesis of HFt-PAS-DOXO constructs. Only five of the 24 PAS-fused HFt N-termini are shown, for clarity.

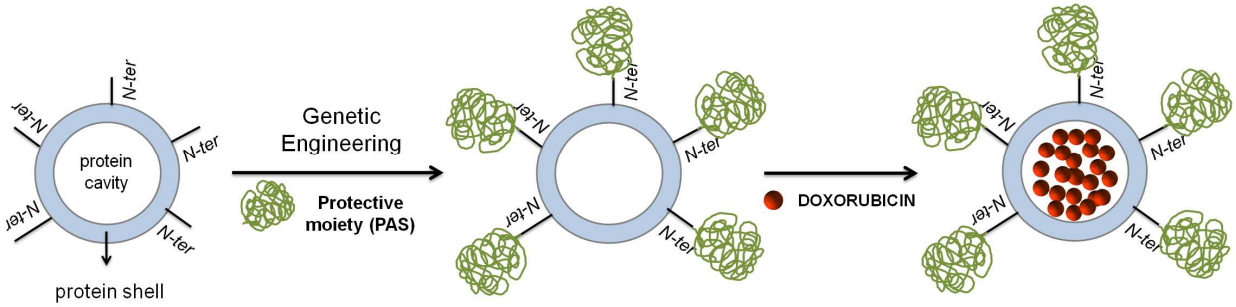

RESULTS AND DISCUSSION

Design and production of HFt-PAS40 and Hft-PAS75 fusion proteins. The goal of this study was to develop a HFt-based delivery system with improved drug encapsulation and pharmacokinetic properties with respect to HFt-based systems developed until now, and suitable for *in vivo* applications. To achieve this purpose, we have developed a novel construct, HFt-PAS, formed by 2 distinct modules genetically linked to each other: a PAS (i.e., rich in proline (P), alanine (A) and serine (S) residues) polypeptide sequence at the N-terminus, and the HFt gene at

the C-terminus (Scheme 1). PASylation technology has been recently described to extend plasma half-life of biopharmaceuticals. In this work, we used PAS sequences both because of their bloodstream stabilizing/protective properties and to increase doxorubicin (DOXO) encapsulation by the HFt nanocarrier.

As a first step to design the HFt-PAS constructs, we built a molecular model of the HFt-PEG variant reported in Vannucci et al.,[4] which was endowed with a suitable hydrodynamic volume for *in vivo* applications. The HFt-PEG variant contains 110 PEG units chemically linked to the -SH groups exposed on the HFt surface. HFt-bonded PEG polymers were modelled in a conformation tightly packed on the protein surface, to reflect the hydrodynamic volume that had been experimentally measured for long circulating PEGylated (PEG 5 kDa) HFt molecules.[4] Then we built several alternative models of HFt-PAS variants, differing in the length of the PAS polymers linked to the exposed N-terminal end of each HFt subunit via three glycine residues. Each of the PAS polymers was modelled in two different conformations, namely fully folded and fully extended, to calculate the minimum and maximum value of hydrodynamic volume potentially assumed by each HFt-PAS construct. The two PASylated constructs having hydrodynamic volumes most similar to the modelled HFt-PEG were HFt-PAS40 and HFt-PAS75, comprising 40-residue PAS polymers in the fully extended conformation and 75-residue PAS polymers in the fully folded conformation, respectively. The shorter length of the fully folded PAS polymer with respect to the fully folded PEG is due to the fact that, because of the presence of peptide bonds and proline residues, PAS polymers have reduced degrees of freedom with respect to the highly flexible PEG.

The fusion proteins HFt-PAS40 and HFt-PAS75 obtained via recombinant protein technology were successfully purified at high yields (100 mg per *E. coli* liter) as soluble fractions of the *E. coli* growth, since they are both highly soluble and stable in aqueous solutions. Noteworthy, in

SDS gel chromatography experiments the PASylated proteins migrated at higher molecular weight masses than expected (Figure 1). In particular, HFt-PAS75 migrated at about 45 kDa compared with a calculated mass of 28 kDa, whereas HFt-PAS40 migrated at about 36 kDa compared with a calculated mass of 25 kDa. This behaviour is in agreement with previous reports on PASylated proteins and has been ascribed to their reduced binding of SDS, whose negatively charged sulfate head group normally provides the electrophoretic driving force. [23-24]

Finally, for comparison purposes, the HFt-PEG variant was synthesized via site-specific maleimide coupling of PEG 5 kDa, as reported by ourselves in Vannucci et al.[4]

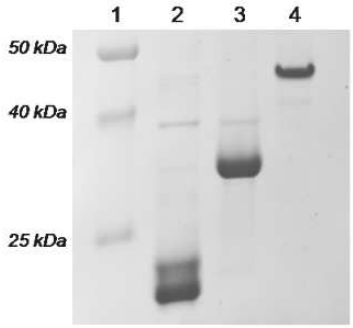

Figure 1. SDS-PAGE band migration profiles of the HFt-PAS proteins. Lane 1 marker; Lane 2 wild-type HFt (1 mg/mL); Lane 3, HFt-PAS40 (1 mg/mL); Lane 4, HFt-PAS75 (1 mg/mL).

Biophysical characterization of HFt-PAS proteins. The hydrodynamic volume of the HFt-PAS40 and HFt-PAS75 fusion proteins was analysed by size-exclusion chromatography (SEC) and dynamic light scattering (DLS) experiments. All samples were found to be highly monodispersed in solution (Figure 2). Both experiments indicated that the PASylated samples actually have similar size to that of HFt-PEG, as well as significantly different elution volumes and sizes with respect to the wild-type HFt, the mean diameters of HFt, HFt-PEG, HFt-PAS40 and HFt-PAS75 being 13.0, 19.0, 17.0 and 20.0 nm, respectively.

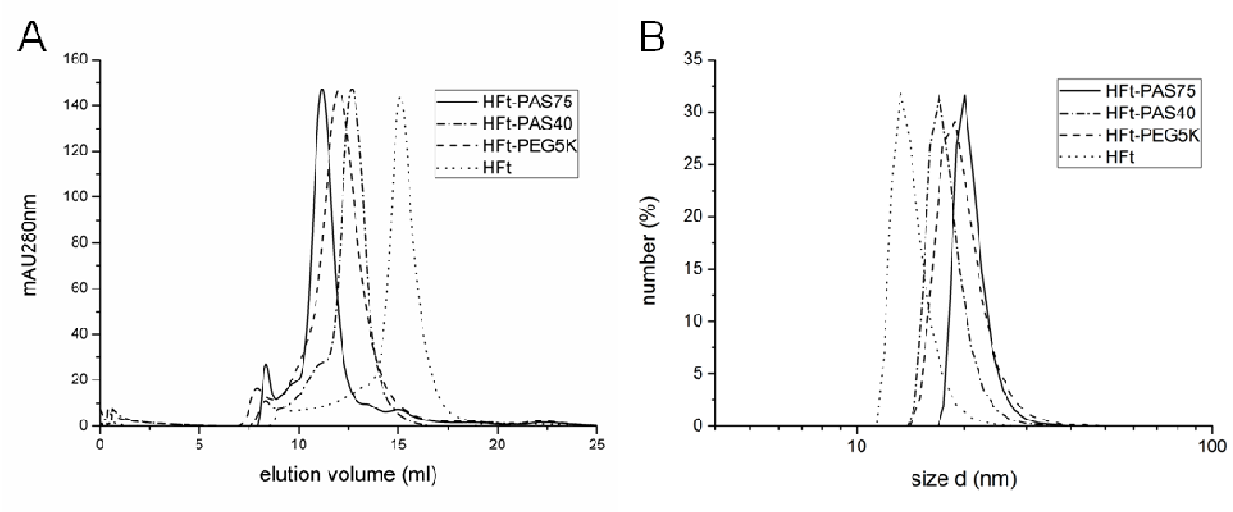

Figure 2. Gel-filtration elution profiles and particle size distribution of HFt-based constructs. (A) Size-exclusion chromatography and (B) dynamic light scattering profiles of HFt-PAS75 (solid line), HFt-PAS40 (dash-dotted lines), HFt-PEG5kDa (dashed line) and HFt (dotted lines).

In principle, N-terminal end modifications may affect the attainment of fully soluble and correctly folded and assembled protein products after overexpression in *E. coli*. Therefore, we decided to investigate the overall assembly of HFt-PAS constructs by transmission electron microscopy (TEM) experiments. TEM images revealed that the PASylated constructs retain the native HFt ability to adopt a spherical cage-like structure (Figure 3).

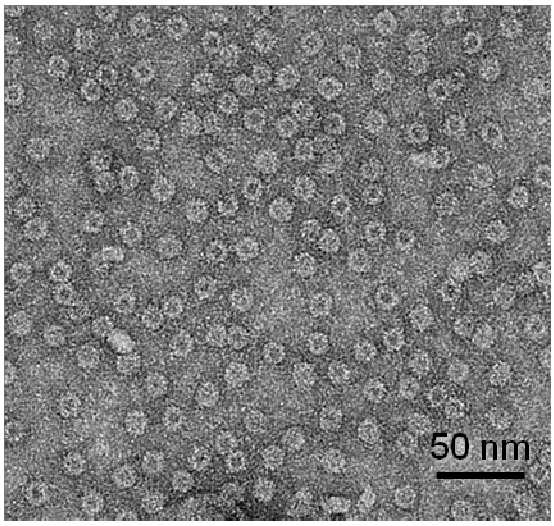

Figure 3. Representative TEM image of negatively stained HFt-PAS75 showing the spherical cage-like assembly typical of ferritin proteins.

To gain further information on the conformational properties of HFt-PAS proteins, circular dichroism (CD) spectra were recorded in the far UV region (Figure 4). The CD spectrum of wild-type HFt exhibited the typical features of an α-helical protein with two characteristic minima around 210 and 220 nm. The spectra of the HFt-PAS proteins revealed a deviation in the first peak at 210 nm, which became more negative (Figure 3). This phenomenon is more evident with HFt-PAS75, and is clearly accountable to the increase of the percentage in random coil conformation due to the presence of unstructured PAS polymers.

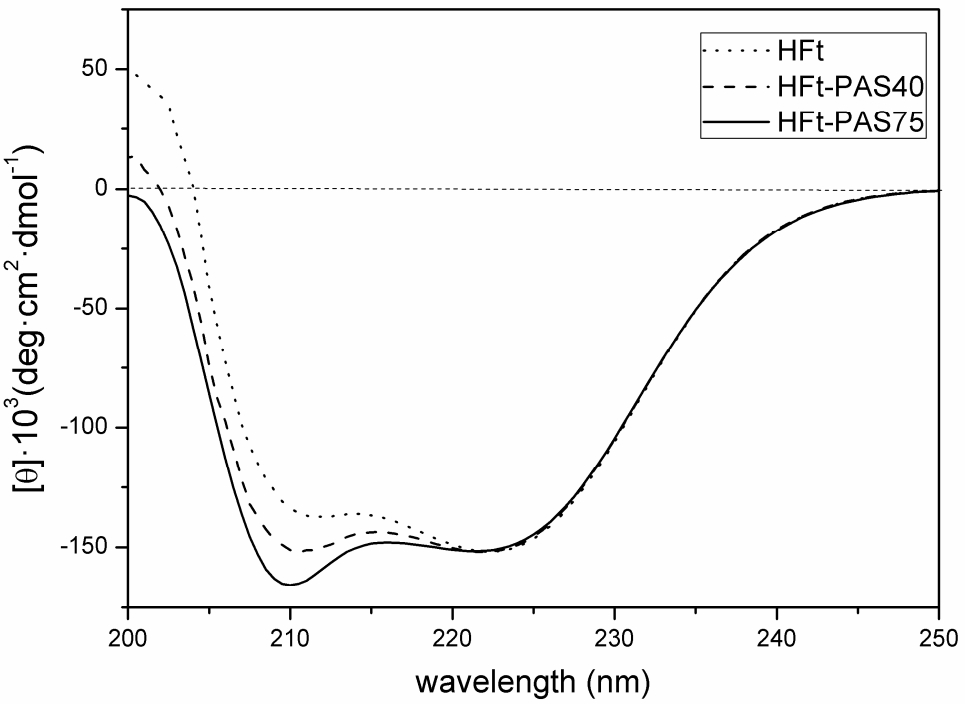

Figure 4. CD spectra of HFt and its PASylated variants. Spectra were recorded at 1 mg/mL protein concentration in 15 mM phosphate buffer and 25°C in a 0.1 cm quartz cuvette, and normalized to the molar ellipticity for each protein.

Doxorubicin encapsulation in HFt-PAS nanocarriers. DOXO was encapsulated inside the protein cavity using the previously reported disassembly/reassembly method (see experimental section). Using this method, about 20-30 molecules of DOXO have been reported to be encapsulated into the ferritin cavity.[2, 7, 20-21] However, a considerable amount of both protein and DOXO precipitated during and at the end of the reaction.[2, 22] We carried-out DOXO encapsulation experiments in our HFt-PAS derivatives using wild-type HFt as control, and DOXO loading by all these variants was demonstrated by UV-visible spectroscopy and size-exclusion chromatography. The amount of encapsulated DOXO was determined as described in the experimental section. Typical SEC elution profiles for HFt-PAS40-DOXO and HFt-PAS75-DOXO are shown in Figure 5A and the relative HFt-DOXO complex recovery and drug loading capacities are presented in

Table I. These results clearly highlight that PASylation dramatically improves HFt ability to encapsulate DOXO, HFt-PAS75 and HFt-PAS40 being able to encapsulate up to 90 and 85 DOXO molecules per protein molecule, respectively. Further, wild-type HFt recovery was ~ 40 %, whereas recovery of PASylated proteins increased to above 95 %.

TABLE I. Yields of doxorubicin encapsulation by HFt-based nanocarriers.
Means of 3 independent repeats ± standard deviations are presented.

Protein	**Protein recovery (%)**	**Number of encapsulated DOXO molecules**
HFt-PAS75 (this study)	96±4	90±4
HFt-PAS40 (this study)	95±3	85±5
HFt (this study)	40±4	29±3
HFt (Ref.[2])	53.33	11
HFt (Ref. [6], a different encapsulation method was used)	n.a.	33
HFt (Ref. [7])	n.a.	28.3
horse spleen ferritin (Ref. [22])	48±9	23±3

n.a., not available.

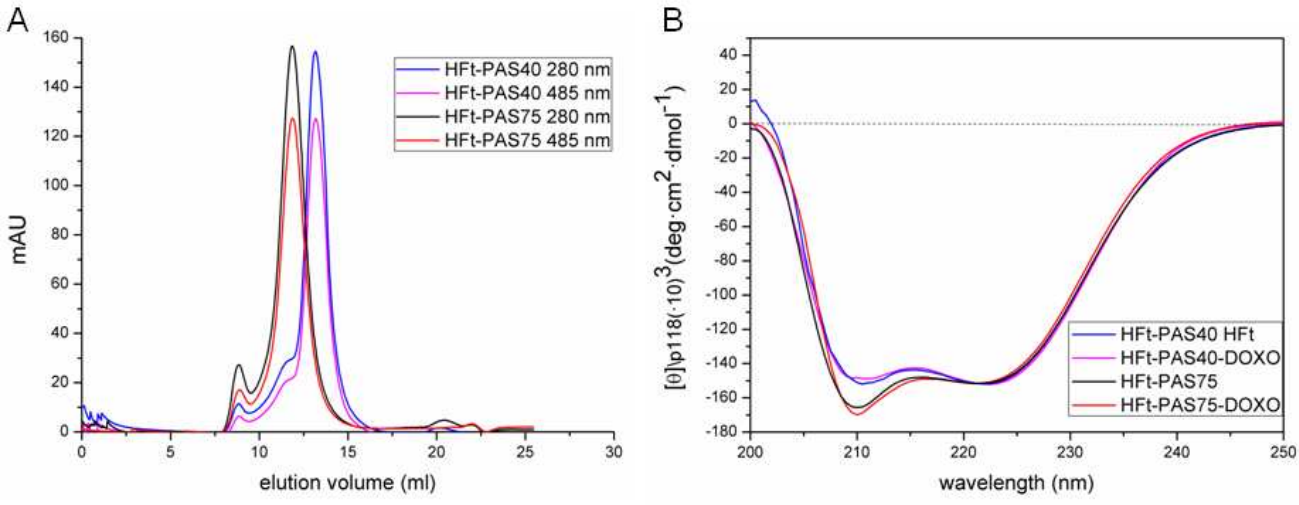

Figure 5. Doxorubicin-encapsulating HFt-based nanocarriers. (A) SEC of HFt-PAS-DOXO constructs. Elution profiles were obtained following simultaneously protein and DOXO contributions at 280 and 485 nm, respectively. (B) CD spectra of HFt-PAS-DOXO constructs showing no secondary structure changes of the HFt protein cage after DOXO loading.

Stability of HFt-PAS-DOXO nanocarriers. To investigate putative HFt-PAS conformational changes occurring after DOXO encapsulation, CD analysis in the far UV region was carried out. The CD spectra of HFt-PAS75-DOXO and HFt-PAS40-DOXO were almost identical to those of the proteins without DOXO (Figure 5B), indicating that DOXO loading does not affect the conformation of the HFt cage.

Then, DOXO release by the HFt-DOXO complexes was evaluated at different time points (every 7 days for 3 months) by incubating them in PBS pH 7.4 at either 4 °C or 37 °C, and monitored for DOXO content by SEC. A huge difference in drug release % between PASylated and non-PASylated HFt variants was observed. HFt-DOXO released DOXO quite rapidly; after two weeks more than 50% of the drug had leaked out from the solution. In contrast, over the same time period, both HFt-PAS proteins showed significantly higher stability, their drug release being lower

than 10% (Figure 6). In addition, after two weeks of storage HFt-DOXO samples presented evident turbidity, which did not allow further measurements at longer times. Importantly, even after 3 months of storage at 4°C HFt-PAS-DOXO complexes displayed neither turbidity nor precipitation and a drug release of about 10%.

These results clearly indicated that genetic fusion of HFt with PAS molecules of appropriate length produced constructs with superior doxorubicin-encapsulation capacity and stability, fostering us to perform *in vivo* pharmacokinetic experiments.

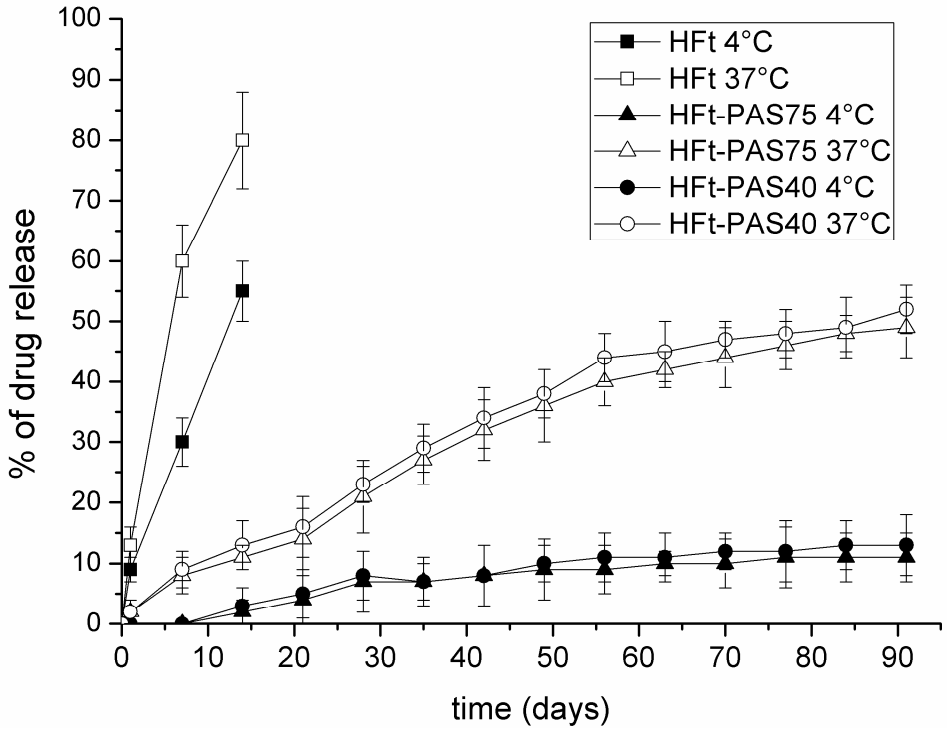

Figure 6. Drug release from HFt-DOXO and HFt-PAS-DOXO complexes. DOXO-containing HFt, HFt-PAS40 and HFt-PAS75 were kept at 4 and 37 °C in PBS pH 7.4, and evaluated by SEC at given time intervals by following simultaneously the 280 and 485 nm wavelengths. The percentage of DOXO leakage was calculated by SEC elution profile comparisons. After 2 weeks, no further measurements could be carried-out for HFt-DOXO complexes due to significant material precipitation.

***In vitro* antiproliferative effects of HFt-PAS-DOXO nanocarriers.** To assess *in vitro* the efficacy of our drug loaded nanosystem to intoxicate and to kill cancer cells we have performed XTT assay on a human pancreatic cancer cell line, PaCa44 cells; we have decided to work with these cell line because PaCa44 cells are less responsive to treatment with conventional chemotherapeutic drugs.[26] The aim was to demonstrate that after encapsulation our drug, DOXO, preserved its pharmacological activity. As summarized in Figure 7 the IC50 of the drug alone was 0.24 μM and the IC50 of our nanosystems were quite superimposable (i.e. IC50 of 0.11 μM for both HFt-PAS40-DOXO and HFt-PAS75-DOXO). These results are of great value in view of potential therapeutic applications, and particularly striking considering that the IC50 reported for the novel and more active *in vivo* formulation of DOXO, the human serum albumin(HSA)-doxorubicin conjugate INNO-206, was reported to be 6.3 μM, ~ 20 fold lower with respect to the naked DOXO *in vitro* (IC50 of 0.3 μM).[27] Nevertheless, INNO-206 showed increased efficacy with respect to DOXO when used *in vivo* due to better pharmacokinetic properties of the albumin carrier.[25]

Although the cancer cell line used for those experiments was a human pancreatic cancer line (MIA-PaCa2) different from that used by ourselves (PaCa44), these two lines have a similar response and IC50 to the naked DOXO in the range of 0.2-0.3 μM.

Moreover, it is important to point out that our nanocage in the form of drug-free compound (i.e. HFt-PAS40) did not show any sign of toxicity in our assay (i.e. viability ≥100%).

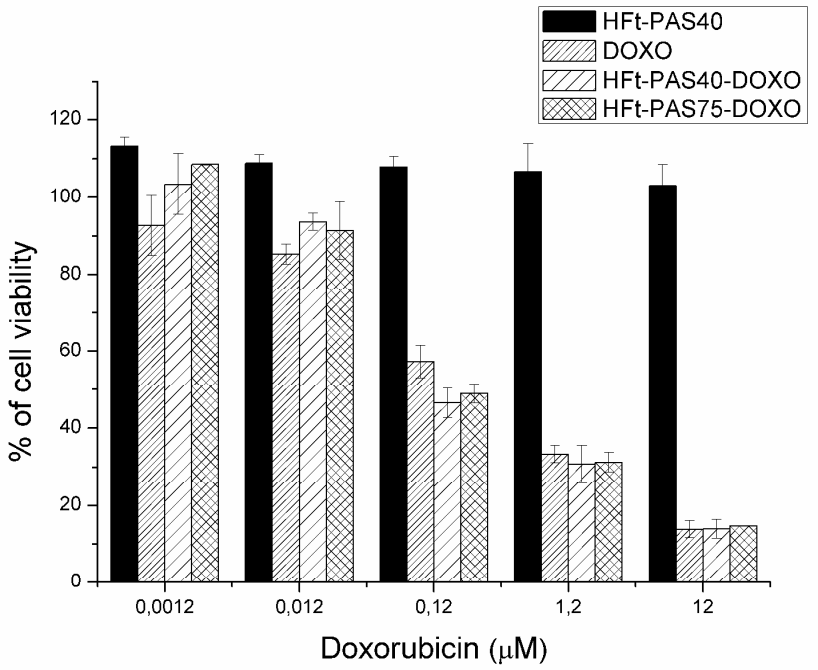

Figure 7. Cell viability of human pancreatic cancer cell line PaCa44 treated with DOXO and DOXO-containing compounds. Cells were incubated for 24 hours with serial dilution of the free drug or the nanosystems under investigation. After 24 hours the supernatant was removed, changed with new medium and the incubation prolonged for other 72 hrs. During the last 3 hours of incubation cell viability was analyzed by XTT assay (i.e. total assay 96 hours). The percent of cell viability was estimated analyzing the values obtained from treated cells with respect to mock treated cells.

Plasma pharmacokinetics (PK) of the HFt-PAS-DOXO nanocarriers *in vivo.* The pharmacokinetic (PK) behaviour of HFt-PAS40-DOXO and HFt-PAS75-DOXO was investigated in an animal system and compared with HFt-DOXO and the free drugs DOXO and INNO-206 (DOXO doses of 5 mg/Kg were used for all the samples).

Results shown in Figure 8 indicate that HFt-PAS polypeptides had a strongly reduced *in vivo* clearance in comparison with wild-type HFt, in accordance with their larger hydrodynamic volume

(Figure 2). In fact, the half-life of DOXO carried by HFt-PAS40 and HFt-PAS75 (i.e., 12.3±0.42 h and 15.6±0.55 h, respectively) is significantly longer than that of DOXO alone (0.28±0.03 h), encapsulated by wild-type HFt (HFt-DOXO: 2.7±0.3 h) or conjugated to serum albumin (INNO-206: 10.9±0.38 h).

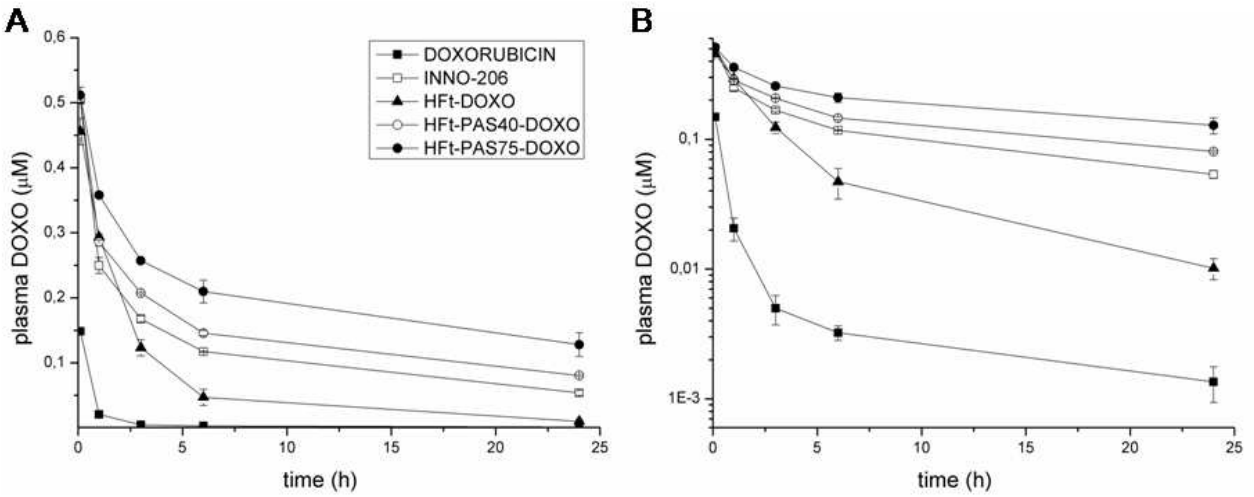

Figure 8. Plasma pharmacokinetics of HFt-PAS-DOXO nanocarriers. Plasma concentrations of DOXO at different time points (10, 60, 180, 360 and 1440 minutes) after *i.v.* injection into healthy nude mice of free drugs, DOXO or INNO-206, or HFt-DOXO, HFt-PAS40-DOXO or HFt-PAS75-DOXO nanocarriers. DOXO concentration in plasma was quantified as described in the experimental section and plotted against the time of sampling (A). Plasma concentration values were also plotted in a semi-logarithmic fashion (B).

Interestingly, PAS sequences previously reported to positively affect the PK properties of biopharmaceutical compounds usually comprise 200-600 residues, the best results being obtained using 600 residue long PAS segments.[23-24] The high *in vitro* and *in vivo* stabilizing effects obtained with the short PAS sequences (i.e., 40 and 75 residue long, respectively) used in this work may be ascribed to the peculiar multivalency of HFt, which is formed by 24 subunits auto-assembled in a

spherical cage. The long plasma half-lives of our HFt-PAS-DOXO complexes are likely to facilitate time-dependent large drug accumulation in tumors, with a significant improvement also in the therapeutic efficacy. These last aspects are currently under investigation by our group.

CONCLUSIONS

We have generated the first, to our knowledge, ferritin protein nanocarrier genetically fused with PAS polypeptides (HFt-PAS). This system incorporates specific features that make the final product potentially useful as a nanocarrier for cancer drug-delivery. Additionally, HFt-PAS is a genetic construct that can be expressed as a single protein product with no additional coupling and/or separation steps required.

Two different HFt-PAS constructs, comprising PAS segments of different length, were designed and expressed at high yields in *E. coli*. Both constructs resulted to be fully assembled and highly stable in both buffers and plasma, and able to encapsulate up to 90 molecules of doxorubicin in the internal cavity. The stability of HFt-PAS-DOXO complexes was dramatically increased and the *in vivo* circulation time considerably longer with respect to wild-type HFt, with PK profiles superior even to the albumin-conjugated DOXO formulation INNO-206. Moreover our DOXO-loaded nanocages preserved the pharmacological activity of the drug while the unloaded nanosystems showed no sign of toxicity as demonstrated by performing a viability *in vitro* assay.

All of the above provides solid evidence supporting the exploitation of long-circulating HFt-PAS nanocarrier described herein in cancer therapy.

ASSOCIATED CONTENT

Supporting Information. Supporting Figure 1 and 2 are available in the Supporting Information. "This material is available free of charge via the Internet at http://pubs.acs.org.".

AUTHOR INFORMATION

Corresponding Author

* Dr. Pierpaolo Ceci, email: pierpaolo.ceci@cnr.it

* Dr. Elisabetta Falvo, email: elisabetta.falvo@uniroma1.it

Author Contributions

The manuscript was written through contributions of all authors. All authors have given approval to the final version of the manuscript.

ACKNOWLEDGMENT

We would like to thank Prof. A. Scarpa (Department of Diagnostics and Public Health University of Verona, Italy) for providing the cell line PaCa44. This research was supported by grants from the Italian Ministry of Economy and Finance Project “FaReBio di Qualità” (P.C.), MIUR flagship Project "Nanomax" (A.B.), Associazione Italiana per la Ricerca sul Cancro (AIRC) I.G: Grant 14204 (P.G.).

G.F. gratefully acknowledges Fondazione Cariverona, Verona Nanomedicine Initiative and Italian Minister of Health RF-2010-2305526 for supporting this work. G.T. gratefully acknowledges AIRC Special Program Molecular Clinical Oncology, 5x1000, (No. 12214).

REFERENCES

1. Falvo, E.; Tremante, E.; Fraioli, R.; Leonetti, C.; Zamparelli, C.; Boffi, A.; Morea, V.; Ceci, P.; Giacomini, P., Antibody-drug conjugates: targeting melanoma with cisplatin encapsulated in protein-cage nanoparticles based on human ferritin. *Nanoscale* **2013,** 5, (24), 12278-85.
2. Zhen, Z.; Tang, W.; Chen, H.; Lin, X.; Todd, T.; Wang, G.; Cowger, T.; Chen, X.; Xie, J., RGD-Modified Apoferritin Nanoparticles for Efficient Drug Delivery to Tumors. *Acs Nano* **2013,** 7, (6), 4830-7.
3. Fan, K.; Cao, C.; Pan, Y.; Lu, D.; Yang, D.; Feng, J.; Song, L.; Liang, M.; Yan, X., Magnetoferritin nanoparticles for targeting and visualizing tumour tissues. *Nat Nanotechnol* **2012,** 7, (7), 459-64.
4. Vannucci, L.; Falvo, E.; Fornara, M.; Di Micco, P.; Benada, O.; Krizan, J.; Svoboda, J.; Hulikova-Capkova, K.; Morea, V.; Boffi, A.; Ceci, P., Selective targeting of melanoma by PEG-masked protein-based multifunctional nanoparticles. *Int J Nanomedicine* **2012,** 7, 1489-509.

5. Vannucci, L.; Falvo, E.; Failla, C. M.; Carbo, M.; Fornara, M.; Canese, R.; Cecchetti, S.; Rajsiglova, L.; Stakheev, D.; Krizan, J.; Boffi, A.; Carpinelli, G.; Morea, V.; Ceci, P., In Vivo Targeting of Cutaneous Melanoma Using an Melanoma Stimulating Hormone-Engineered Human Protein Cage with Fluorophore and Magnetic Resonance Imaging Tracers. *Journal of Biomedical Nanotechnology* **2015,** 11, (1), 81-92.
6. Liang, M.; Fan, K.; Zhou, M.; Duan, D.; Zheng, J.; Yang, D.; Feng, J.; Yan, X., H-ferritin-nanocaged doxorubicin nanoparticles specifically target and kill tumors with a single-dose injection. *Proc Natl Acad Sci U S A* **2014,** 111, (41), 14900-5.
7. Bellini, M.; Mazzucchelli, S.; Galbiati, E.; Sommaruga, S.; Fiandra, L.; Truffi, M.; Rizzuto, M. A.; Colombo, M.; Tortora, P.; Corsi, F.; Prosperi, D., Protein nanocages for self-triggered nuclear delivery of DNA-targeted chemotherapeutics in Cancer Cells. *J Control Release* **2014,** 196, 184-96.
8. Heger, Z.; Skalickova, S.; Zitka, O.; Adam, V.; Kizek, R., Apoferritin applications in nanomedicine. *Nanomedicine-Uk* **2014,** 9, (14), 2233-2245.
9. Bellapadrona, G.; Sinkar, S.; Sabanay, H.; Liljestrom, V.; Kostiainen, M.; Elbaum, M., Supramolecular Assembly and Coalescence of Ferritin Cages Driven by Designed Protein-Protein Interactions. *Biomacromolecules* **2015,** 16, (7), 2006-11.
10. Kang, Y. J.; Park, D. C.; Shin, H. H.; Park, J.; Kang, S., Incorporation of Thrombin Cleavage Peptide into a Protein Cage for Constructing a Protease-Responsive Multifunctional Delivery Nanoplatform. *Biomacromolecules* **2012,** 13, (12), 4057-4064.
11. Schoonen, L.; van Hest, J. C., Functionalization of protein-based nanocages for drug delivery applications. *Nanoscale* **2014,** 6, (13), 7124-41.
12. Romagnani, S., Immunological tolerance and autoimmunity. *Intern Emerg Med* **2006,** 1, (3), 187-196.
13. Uchida, M.; Willits, D. A.; Muller, K.; Willis, A. F.; Jackiw, L.; Jutila, M.; Young, M. J.; Porter, A. E.; Douglas, T., Intracellular Distribution of Macrophage Targeting Ferritin-Iron Oxide Nanocomposite. *Adv Mater* **2009,** 21, (4), 458-462.
14. Crich, S. G.; Bussolati, B.; Tei, L.; Grange, C.; Esposito, G.; Lanzardo, S.; Camussi, G.; Aime, S., Magnetic resonance visualization of tumor angiogenesis by targeting neural cell adhesion molecules with the highly sensitive gadolinium-loaded apoferritin probe. *Cancer Research* **2006,** 66, (18), 9196-9201.
15. Lin, X.; Xie, J.; Niu, G.; Zhang, F.; Gao, H.; Yang, M.; Quan, Q.; Aronova, M. A.; Zhang, G.; Lee, S.; Leapman, R.; Chen, X., Chimeric ferritin nanocages for multiple function loading and multimodal imaging. *Nano Lett* **2011,** 11, (2), 814-9.
16. Fantechi, E.; Innocenti, C.; Zanardelli, M.; Fittipaldi, M.; Falvo, E.; Carbo, M.; Shullani, V.; Di Cesare Mannelli, L.; Ghelardini, C.; Ferretti, A. M.; Ponti, A.; Sangregorio, C.; Ceci, P., A smart platform for hyperthermia application in cancer treatment: cobalt-doped ferrite nanoparticles mineralized in human ferritin cages. *Acs Nano* **2014,** 8, (5), 4705-19.
17. Liu, X. Y.; Wei, W.; Huang, S. J.; Lin, S. S.; Zhang, X.; Zhang, C. M.; Du, Y. G.; Ma, G. H.; Li, M.; Mann, S.; Ma, D., Bio-inspired protein-gold nanoconstruct with core-void-shell structure: beyond a chemo drug carrier. *J Mater Chem B* **2013,** 1, (25), 3136-3143.
18. Bode, S. A.; Minten, I. J.; Nolte, R. J.; Cornelissen, J. J., Reactions inside nanoscale protein cages. *Nanoscale* **2011,** 3, (6), 2376-89.
19. Li, L.; Fang, C. J.; Ryan, J. C.; Niemi, E. C.; Lebron, J. A.; Bjorkman, P. J.; Arase, H.; Torti, F. M.; Torti, S. V.; Nakamura, M. C.; Seaman, W. E., Binding and uptake of H-ferritin are mediated by human transferrin receptor-1. *Proc Natl Acad Sci U S A* **2010,** 107, (8), 3505-10.
20. Gumulec, J.; Fojtu, M.; Raudenska, M.; Sztalmachova, M.; Skotakova, A.; Vlachova, J.; Skalickova, S.; Nejdl, L.; Kopel, P.; Knopfova, L.; Adam, V.; Kizek, R.; Stiborova, M.; Babula, P.; Masarik, M., Modulation of Induced Cytotoxicity of Doxorubicin by Using Apoferritin and Liposomal Cages. *International Journal of Molecular Sciences* **2014,** 15, (12), 22960-22977.
21. Zhang, L. B.; Li, L.; Di Penta, A.; Carmona, U.; Yang, F.; Schops, R.; Brandsch, M.; Zugaza, J. L.; Knez, M., H-Chain Ferritin: A Natural Nuclei Targeting and Bioactive Delivery Nanovector. *Adv Healthc Mater* **2015,** 4, (9), 1305-1310.
22. Kilic, M. A.; Ozlu, E.; Calis, S., A Novel Protein-Based Anticancer Drug Encapsulating Nanosphere: Apoferritin-Doxorubicin Complex. *Journal of Biomedical Nanotechnology* **2012,** 8, (3), 508-514.
23. Schlapschy, M.; Binder, U.; Borger, C.; Theobald, I.; Wachinger, K.; Kisling, S.; Haller, D.; Skerra, A., PASylation: a biological alternative to PEGylation for extending the plasma half-life of pharmaceutically active proteins. *Protein Eng Des Sel* **2013,** 26, (8), 489-501.
24. Harari, D.; Kuhn, N.; Abramovich, R.; Sasson, K.; Zozulya, A. L.; Smith, P.; Schlapschy, M.; Aharoni, R.; Koster, M.; Eilam, R.; Skerra, A.; Schreiber, G., Enhanced in Vivo Efficacy of a Type I

Interferon Superagonist with Extended Plasma Half-life in a Mouse Model of Multiple Sclerosis. *J Biol Chem* **2014,** 289, (42), 29014-29029.
25. Unger, C.; Haring, B.; Medinger, M.; Drevs, J.; Steinbild, S.; Kratz, F.; Mross, K., Phase I and pharmacokinetic study of the (6-maleimidocaproyl)hydrazone derivative of doxorubicin. *Clin Cancer Res* **2007,** 13, (16), 4858-66.
26. Monti, P.; Marchesi, F.; Reni, M.; Mercalli, A.; Sordi, V.; Zerbi, A.; Balzano, G.; Di Carlo, V.; Allavena, P.; Piemonti, L., A comprehensive in vitro characterization of pancreatic ductal carcinoma cell line biological behavior and its correlation with the structural and genetic profile. *Virchows Arch* **2004,** 445, (3), 236-47.
27. Kratz, F.; Azab, S.; Zeisig, R.; Fichtner, I.; Warnecke, A., Evaluation of combination therapy schedules of doxorubicin and an acid-sensitive albumin-binding prodrug of doxorubicin in the MIA PaCa-2 pancreatic xenograft model. *Int J Pharm* **2013,** 441, (1-2), 499-506.

Table of Contents